

Structural and dielectric properties of $\text{Ba}_{0.85}\text{Sr}_{0.15}(\text{Zr}_{0.18}\text{Ti}_{0.82})\text{O}_3$ thin films grown by a sol–gel process

Jiwei Zhai^{a,*}, Xi Yao^a, Haydn Chen^b

^a Functional Materials Research Laboratory, Tongji University, Shanghai 200092, China

^b Department of Physics and Materials Science, City University of Hong Kong, Kowloon, Hong Kong, China

Received 4 December 2003; received in revised form 9 December 2003; accepted 22 December 2003

Available online 30 April 2004

Abstract

The $\text{Ba}_{0.85}\text{Sr}_{0.15}\text{Zr}_{0.18}\text{Ti}_{0.82}\text{O}_3$ (BSZT) thin films were deposited via sol–gel process on LaNiO_3 -coated silicon substrates. The grain size decreased and the microstructure became dense when substitute Zr for Ti. Dielectric properties were investigated as a function of temperature, frequency and direct current electric field. The temperature dependent dielectric measurements revealed that the thin films have diffuse phase transition characteristics. The tunability of $\text{Ba}_{0.8}\text{Sr}_{0.2}\text{Sn}_{0.10}\text{Ti}_{0.90}\text{O}_3$ thin films is about 57%, at an applied field of 415 kV/cm and measurement frequency of 1 MHz. It was observed that the leakage current density of $\text{Ba}_{0.85}\text{Sr}_{0.15}\text{Zr}_{0.18}\text{Ti}_{0.82}\text{O}_3$ is higher than that of BZT thin films.

© 2004 Elsevier Ltd and Techna Group S.r.l. All rights reserved.

Keywords: B. Microstructure; C. Dielectric properties; BSZT thin film; Phase transition

1. Introduction

A large number of lead-free BaTiO_3 -based ceramics were studied in recent years. Depending on the composition, some of them exhibit a relaxor behavior whose characteristics were related to the type of ionic substitution and to the substitution rate. Some of these materials could prove valuable because they are environment-friendly. Barium zirconium titanate $\text{BaZr}_{1-y}\text{Ti}_y\text{O}_3$ -based (BZT) ceramics is a solid solution compound that exhibits paraelectric or ferroelectric properties depending on the specific composition and temperature [1,2]. The dielectric constant of BZT can also be controlled electrically by applying a direct current (DC) electric field bias across it. Field dependent dielectric constant of BZT may be exploited for radio frequency (RF) and microwave tunable filter applications [3,4].

There have been some efforts to replace the BST films with new films such as $\text{Ba}_{0.85}\text{Sr}_{0.15}\text{Zr}_{0.18}\text{Ti}_{0.82}\text{O}_3$ (BSZT) etc. In case of BSZT, it is obtained by substituting ions at the B site and A site of the BaTiO_3 with Zr and Sr in compounds of the perovskite structure ABO_3 . It is reported

that an increase in the Zr content induces a reduction in the average grain size, decreases the dielectric constant, and maintains a leakage current low and stable.

In this paper, we reported on the $\text{Ba}_{0.85}\text{Sr}_{0.15}\text{Zr}_{0.18}\text{Ti}_{0.82}\text{O}_3$ thin films deposition on LaNiO_3 as buffer layer Pt/Ti/ SiO_2 /Si substrates and analyze the relationship of microstructure and dielectric behavior of thin films. Electric properties of thin films are studied as a function of frequency, temperature and electric field.

2. Experimental processing

The barium acetate $[\text{Ba}(\text{CH}_3\text{COO})_2]$, strontium acetate $\text{Sr}(\text{CH}_3\text{COO})_2$, zirconium isopropoxide $[\text{Zr}(\text{OC}_3\text{H}_7)_4]$, and titanium isopropoxide $[\text{Ti}(\text{OC}_3\text{H}_7)_4]$ were used as starting materials. Acetic acid was used as solvent. $\text{Ba}(\text{CH}_3\text{COO})_2$ was heated and dissolved in acetic acid. Zirconium isopropoxide and titanium isopropoxide were mixed in a ratio according to a predetermined number (BaTiO_3 , $\text{Ba}_{0.85}\text{Sr}_{0.15}\text{TiO}_3$, $\text{Ba}(\text{Zr}_{18}\text{Ti}_{82})\text{O}_3$, and $\text{Ba}_{0.85}\text{Sr}_{0.15}(\text{Zr}_{18}\text{Ti}_{82})\text{O}_3$), and then dissolved into heated glacial acetic acid. After cooling to room temperature, the ethylene glycol $\text{CH}_2\text{OHCH}_2\text{OH}$ was added to control the viscosity and cracking of films; the solution was mixed

* Corresponding author. Tel.: +86-21-65980544;
fax: +86-21-65985179.
E-mail address: zhajijiwei@eastday.com (J. Zhai).

and refluxed for 1 h. The concentration of the final solution was adjusted to about 0.3 M. After aging the hydrolyzed solution for 24 h, thin-film deposition was carried out on the $\text{LaNiO}_3/\text{Pt}/\text{Ti}/\text{SiO}_2/\text{Si}(100)$ substrates by spin coating at 3000 rpm for 30 s each layer. Each spin-coated BZT layer was subsequently heat treated at 500°C for 5 min. The coating and heat treatment procedures were repeated several times until reaching the desired thickness (about 360 nm). The final anneal at high temperature of 700°C for 30 min crystallize the amorphous films.

The crystalline phase of the thin films was identified by X-ray diffraction (BRUCKER D8 powder diffractometer). The film thickness and the surface morphology were determined by FESEM. For the electrical measurements, the top gold electrode of a $400\ \mu\text{m}$ square was deposited by DC-sputtering. The capacitance–voltage (C – V) and capacitance–temperature (C – T) characteristics were measured using an Agilent 4284A LCR meter. The current–voltage (I – V) characteristics were measured by a HP 4140B. The sample's temperature was varied by using a Delta chamber.

3. Results and discussion

The XRD patterns of (a) BaTiO_3 , (b) $\text{Ba}_{0.85}\text{Sr}_{0.15}\text{TiO}_3$, (c) $\text{Ba}(\text{Zr}_{18}\text{Ti}_{82})\text{O}_3$, and (d) $\text{Ba}_{0.85}\text{Sr}_{0.15}(\text{Zr}_{18}\text{Ti}_{82})\text{O}_3$ thin films were shown in Fig. 1. It is evident that these films were perovskite phase. It was seen that when the films are deposited on $\text{LaNiO}_3/\text{Pt}/\text{Ti}/\text{SiO}_2/\text{Si}(100)$ substrate, (100) and (200) peaks are corresponded with the intensity of (110) peak. It is evident that the films were perovskite phase and had the (100) preferred orientation. A slight shift of the (200) plane is shown in the inset of the Fig. 1. A shift of 2θ angles to the high angle side when Sr doped BaTiO_3 films reveals the constriction of perovskite lattice by the addition of the

Sr in BaTiO_3 . This constriction of perovskite lattice is related to the fact that the ionic radius of Sr^{2+} is smaller than that of Ba^{2+} . Substitution of Ti by Zr leads to an expansion of perovskite lattice in BaTiO_3 thin films which is related to the fact the ionic radius of Zr^{4+} is greater than that of Ti^{4+} . The inset of the Fig. 1 also showed the shift of 2θ angles that were related to the Sr^{2+} for Ba^{2+} as well as Zr^{4+} for Ti^{4+} substitutions.

Fig. 2 shows SEM images of the sol–gel deposited thin films on $\text{LaNiO}_3/\text{Pt}/\text{Ti}/\text{SiO}_2/\text{Si}(100)$. As shown in Fig. 2, all films have subjected to a final anneal at 700°C . The addition of Zr to the BaTiO_3 lattice decreased the grain size of the crystallized films. The decreasing grain size with increasing zirconium may be attributable to lower grain-growth rates from the more slowly diffusion of the Zr^{4+} ion, which has a bigger ionic radius than Ti^{4+} . Crystallization may be initiated earlier with lower zirconium contents, resulting in a larger grain size for the same heat treatment [5]. The addition of Sr and Zr to the BaTiO_3 lattice, the grain size of the crystallized films was larger than that of Zr for Ti substitutions, but smaller than that of BaTiO_3 thin films. The increasing grain size when substitute Sr for Ba may be attributable to higher grain-growth rates from the more rapid diffusion of the Sr^{2+} (0.113 nm) ion, which has a smaller ionic radius than Ba^{2+} (0.135 nm).

Fig. 3 showed the dielectric constant and dielectric loss of thin films $\text{Ba}_{0.85}\text{Sr}_{0.15}\text{Zr}_{0.18}\text{Ti}_{0.82}\text{O}_3$, as function of frequencies. The dielectric constant shows dielectric dispersion typical of the thin films, and low losses are obtained at frequencies up to 500 kHz. The dielectric constant showed a slight tendency, to decrease with higher frequencies, the increasing tendency of dielectric loss was obviously at higher frequency ranges, several possible causes exist for such dispersion, including the hypothesis of the influence of the contact resistance between the probe and the electrode, resonance due to high dielectric constant. Similar frequency dispersion behavior was also reported for other ferroelectric thin films [6,7].

The dielectric constant and loss of thin films $\text{Ba}_{0.85}\text{Sr}_{0.15}\text{Zr}_{0.18}\text{Ti}_{0.82}\text{O}_3$ as a function of temperature and frequency are shown in Fig. 4. Dielectric constant and dielectric loss were measured with an AC field of 0.4 kV/cm and the heating rate was $3^\circ\text{C}/\text{min}$. The ϵ – T characteristics were strongly frequency dependent, especially at the point of phase transformation. Fig. 4 shows the dielectric loss data for the films, indicating the expected relationship between dielectric constant and dielectric loss. It is evident that the phase transition of thin films is between -20 and 30°C and indicated the diffused nature of the film. The broadening of transition together with the shift of the Curie temperature towards higher temperature in thin films of normal ferroelectrics ceramics was due to the influence of the interfaces of the films and the fine grained structure and unrelaxed growth strain [8,9].

Fig. 5 shows the tuning of the capacitance as a function of applied DC voltage for thin films at room temperature. Dielectric constant and dielectric loss of the films was mea-

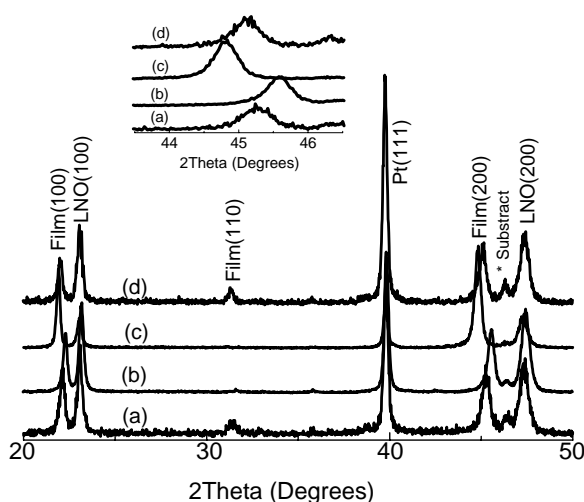


Fig. 1. XRD patterns of sol–gel deposited: (a) BaTiO_3 , (b) $\text{Ba}_{0.85}\text{Sr}_{0.15}\text{TiO}_3$, (c) $\text{Ba}(\text{Zr}_{18}\text{Ti}_{82})\text{O}_3$, and (d) $\text{Ba}_{0.85}\text{Sr}_{0.15}(\text{Zr}_{18}\text{Ti}_{82})\text{O}_3$ thin films.

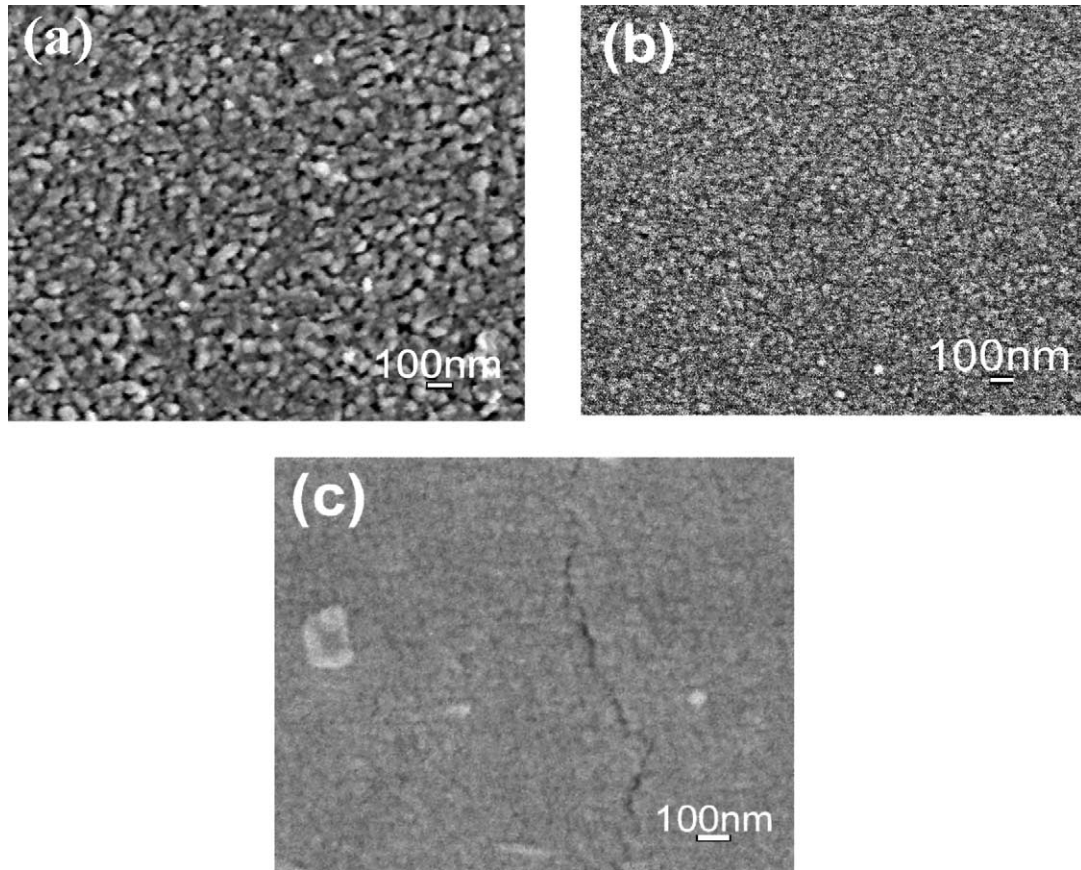


Fig. 2. SEM micrographs of sol-gel deposited: (a) BaTiO_3 , (b) $\text{Ba}(\text{Zr}_{18}\text{Ti}_{82})\text{O}_3$, and (c) $\text{Ba}_{0.85}\text{Sr}_{0.15}(\text{Zr}_{18}\text{Ti}_{82})\text{O}_3$ thin films.

sured at 1 MHz, with an AC field of 0.4 kV/cm superimposed on a slowly varying DC bias field. The DC bias was stepped through 0.2 V intervals and held 1 s prior to capacitance measurement. The loss tangent measurements as a function of bias voltage gave curves of similar sharp to the tuning curves in the range of low DC electric field. The dielectric constant tunability of the films can be expressed as $(\epsilon(0) - \epsilon(E))/\epsilon(0)$. The tunability of $\text{Ba}_{0.85}\text{Sr}_{0.15}\text{Zr}_{0.18}\text{Ti}_{0.82}\text{O}_3$ thin films is about 57%, at an applied field of 415 kV/cm and measurement frequency of 1 MHz. The values of dielectric loss at 1 MHz ranged from ~ 0.035 at zero bias to ~ 0.037 at 415 kV/cm.

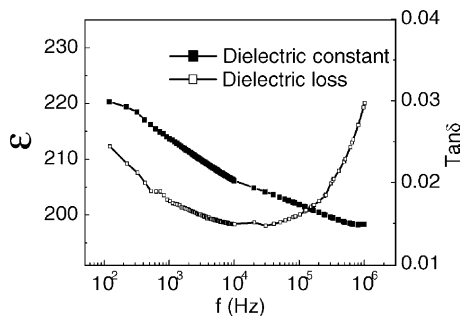


Fig. 3. The dielectric constant and dielectric loss of $\text{Ba}_{0.85}\text{Sr}_{0.15}(\text{Zr}_{18}\text{Ti}_{82})\text{O}_3$ thin films, as a function of frequency.

The difference in the leakage current characteristics of thin film is shown in Fig. 6. It is indicated that the leakage current density of $\text{Ba}_{0.85}\text{Sr}_{0.15}\text{Zr}_{0.18}\text{Ti}_{0.82}\text{O}_3$ is higher than that of BZT thin films. The leakage currents density of thin

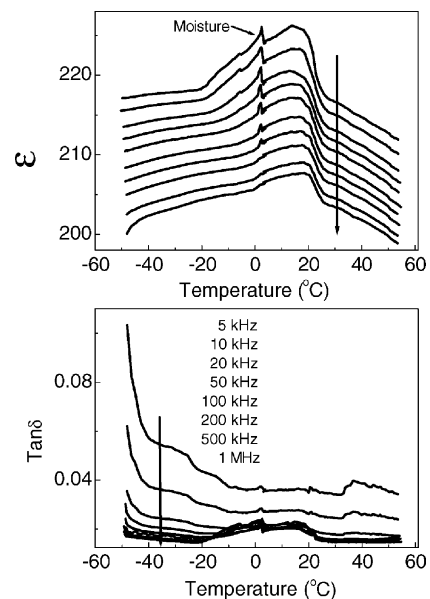


Fig. 4. The dielectric constant and dielectric loss of $\text{Ba}_{0.85}\text{Sr}_{0.15}(\text{Zr}_{18}\text{Ti}_{82})\text{O}_3$ thin films, as a function of temperature and frequency.

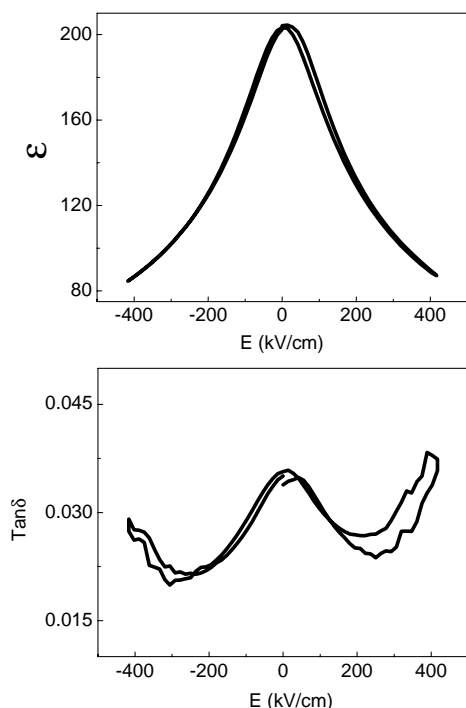


Fig. 5. ϵ - E characteristics of $\text{Ba}_{0.85}\text{Sr}_{0.15}(\text{Zr}_{0.18}\text{Ti}_{0.82})\text{O}_3$ thin films at room temperature (measurement frequency 1 MHz).

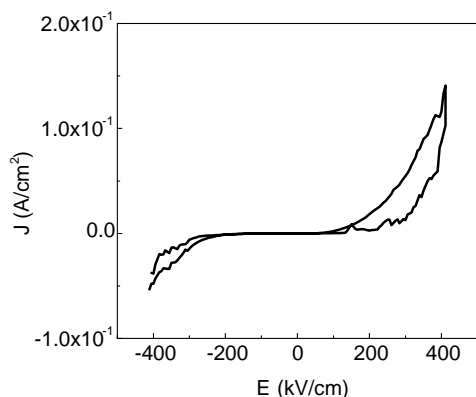


Fig. 6. J - E characteristics of $\text{Ba}_{0.85}\text{Sr}_{0.15}(\text{Zr}_{0.18}\text{Ti}_{0.82})\text{O}_3$ thin films.

films at 100 kV/cm was about $2 \times 10^{-4} \text{ A/cm}^2$. The difference is due to the enhanced ionic polarization and improved crystallinity with larger grain size for the BSZT thin films. The films with larger grain sizes have overall shorter conduction paths along the grain boundaries, which causes an increase in the leakage current.

4. Conclusion

The $\text{Ba}_{0.85}\text{Sr}_{0.15}\text{Zr}_{0.18}\text{Ti}_{0.82}\text{O}_3$ thin films were deposited via sol-gel process on LaNiO_3 -coated silicon substrates. The

films were single perovskite phase and had the (100) preferred orientation. The addition of Zr to the BaTiO_3 lattice decreased the grain size of the crystallized films and the microstructure became dense. The temperature dependent dielectric measurements revealed that the thin films have the diffuse phase transition characteristics. The leakage currents density of thin films at 100 kV/cm was about $2 \times 10^{-4} \text{ A/cm}^2$ and the capacitor tunability of films was 57% at an applied field of 415 kV/cm and measurement frequency of 1 MHz. It was observed that leakage currents increased asymmetrically for the negative and positive bias voltage and the leakage current density of $\text{Ba}_{0.85}\text{Sr}_{0.15}\text{Zr}_{0.18}\text{Ti}_{0.82}\text{O}_3$ is higher than that of BZT thin films due to the fine grain structure for the BZT thin films.

Acknowledgements

This research was supported by the Ministry of Sciences and Technology of China through 973-project under grant 2002CB613304 and the university key studies project of Shanghai.

References

- [1] P. Hansen, D. Hennings, H. Schreinemacher, High- k dielectric ceramics from donor/acceptor-codoped $(\text{Ba}_{1-x}\text{Ca}_x)(\text{Ti}_{1-y}\text{Zr}_y)\text{O}_3$ (BCTZ), *J. Am. Ceram. Soc.* 81 (5) (1998) 1369–1373.
- [2] W.-C. Yi, T.S. Kallkur, E. Philofsky, L. Kammerdiner, A.A. Rywak, Dielectric properties of Mg-doped $\text{Ba}_{0.96}\text{Ca}_{0.04}\text{Ti}_{0.84}\text{Zr}_{0.16}\text{O}_3$ thin films fabricated by metalorganic deposition method, *Appl. Phys. Lett.* 78 (22) (2001) 3517–3519.
- [3] A. Dixit, S.B. Majumder, A. Savvinov, R.S. Katiyar, R. Guo, A.S. Bhalla, Investigations on the sol-gel-derived barium zirconium titanate thin films, *Mater. Lett.* 56 (6) (2002) 933–940.
- [4] T.B. Wu, C.M. Wu, M.L. Chen, Highly insulative barium zirconate-titanate thin films prepared by rf magnetron sputtering for dynamic random access memory applications, *Appl. Phys. Lett.* 69 (18) (1996) 2659–2661.
- [5] M.C. Gust, L.A. Momoda, N.D. Evans, M.L. Mecartney, Crystallization of sol-gel-derived barium strontium titanate thin films, *J. Am. Ceram. Soc.* 84 (5) (2001) 1087–1092.
- [6] R.R. Das, P. Bhattacharya, R.S. Katiyar, Enhanced ferroelectric properties in laser-ablated $\text{SrBi}_2\text{Nb}_2\text{O}_9$ thin films on platinized silicon substrate, *Appl. Phys. Lett.* 81 (9) (2002) 1672–1674.
- [7] F.M. Pontes, D.S.L. Pontes, E.R. Leite, E. Longo, Influence of Ca concentration on the electric, morphological, and structural properties of $(\text{Pb}, \text{Ca})\text{TiO}_3$ thin films, *J. Appl. Phys.* 91 (10) (2002) 6650–6655.
- [8] B. Qu, W. Zhang, P.L. Zhang, Phase-transition behavior of the spontaneous polarization and susceptibility of ferroelectric thin films, *Phys. Rev. B* 52 (2) (1994) 766–770.
- [9] C.B. Parker, J.P. Maria, A.I. Kingon, Temperature and thickness dependent permittivity of $(\text{Ba}, \text{Sr})\text{TiO}_3$ thin films, *Appl. Phys. Lett.* 81 (2) (2002) 340–342.